On the fluorescence enhancement mechanism of Er^{3+} in germanate glass containing silver particles*

Li Xiang-Ping(李香萍)[a)b)], Chen Bao-Jiu(陈宝玖)[a)†], Shen Ren-Sheng(申人升)[b)], Zhang Jin-Su(张金苏)[a)], Sun Jia-Shi(孙佳石)[a)], Cheng Li-Hong(程丽红)[a)], Zhong Hai-Yang(仲海洋)[a)], Tian Yue(田 跃)[a)], Fu Shao-Bo(付少博)[a)], and Du Guo-Tong(杜国同)[b)]

[a)] *Department of Physics, Dalian Maritime University, Dalian* 116026, *China*

[b)] *School of Physics and Optoelectronic Engineering, Dalian University of Technology, Dalian* 116024, *China*

(Received 25 June 2012; revised manuscript received 10 August 2012)

The spectral properties of trivalent erbium ions (Er^{3+}) are systematically studied in a melt-quenched germanate glass (60 GeO_2-20PbO-10BaO-10K_2O-0.1Ag_2O) containing silver (Ag) particles. Thermal treatment of the material leads to the precipitation of Ag particles as observed by transmission electron microscopy and confirmed by absorption spectrum for the obvious surface plasmon resonance peak of Ag particles. The fluorescence from Er^{3+} in the 10-min-annealed sample with Ag particles is found to be 4.2 times enhanced compared with the unannealed sample excited by 488-nm Ar^+ laser. A comparison is made between a spectral study performed on the unannealed Er^{3+}-doped sample and the one annealed for 20 min. The data of absorption cross section and Judd–Ofelt intensity parameters show the agreement between the two samples no matter whether there are Ag particles, indicating that the introduction of Ag particles by post-heat treatment has no effect on the crystal field environment of Er^{3+} ions. The fluorescence enhancement is attributed to the surface plasmon oscillations of Ag particles in germanate glass.

Keywords: Er^{3+}, silver particles, fluorescence enhancement, surface plasmon resonance

PACS: 32.50.+d, 71.20.Eh, 71.15.Qe **DOI:** 10.1088/1674-1056/22/2/023202

1. Introduction

The excitation of surface plasmons (SPs) by light is termed the surface plasmon resonance (SPR) at the surfaces of noble metal films or particles, which has attracted much attention both theoretically and experimentally due to its applications in plasmon biosensors and enhancement of some physical quantities, such as Raman scattering intensities, fluorescence intensities, the absorptions of light in molecules, and the quantum efficiencies of light-emitting materials and light emission diodes (LEDs),[1–11] etc. Up to now, SPs-enhanced Raman scattering and fluorescence have been widely observed in various materials, such as inorganic quantum dots, semiconductors, organic materials, and rare-earth ion-doped materials containing heavy metal particles (Au, Ag).[12–21] It has been reported that the heavy metal SPs can enhance a Raman signal more than 10^8 times,[22] and they increase the fluorescence several times in rare-earth ion-doped materials,[16] which evokes considerable research interest in the interaction between heavy metal particles and light-emitting centers.

Trivalent erbium ion (Er^{3+}), as one of the most important active ions in the rare-earth family due to its favorable energy level structure, has been exploited in a wide variety of glasses for applications in solid-state lasers and optical amplifiers. In recent years, Er^{3+} and Ag co-doped bismuth, germanate, tellurite, and oxyfluoride glasses have been extensively investigated and fluorescence enhancement phenomena have been observed.[23–26] However, it is not clear whether the enhancement results from plasmonic resonance, energy transfer or any other factor.[27] Among all of the above glasses, germanate glass has proved to be one of the promising hosts for such applications due to its high chemical durability and temperature stability; moreover, it has a higher refractive index and lower phonon energy than silicate, borate, and phosphate glasses.

In this paper, Er^{3+}-doped germanate glasses containing Ag particles are prepared by melt-quenching method with post-annealing treatment. Their spectral properties and influences of Ag particles on Er^{3+} luminescence are systematically studied. Fluorescence enhancement is observed, and its physical mechanism is attributed to the SPs oscillations of Ag particles in germanate glass.

2. Experiment

2.1. Sample preparation

Er^{3+}-doped germanate glasses containing small Ag particles with designed composition 60GeO_2-20PbO-10BaO-10K_2O-0.1Ag_2O-1Er_2O_3 (in molar ratio) were prepared by a conventional melt-quenching method. Analytical grade GeO_2,

*Project supported by the National Natural Science Foundation of China (Grant Nos. 61078061 and 11104023), the Natural Science Foundation of Liaoning Province, China (Grant No. 20111032), the State Key Development Program for Basic Research of China (Grant No. 2012CB626801), and the Fundamental Research Funds for the Central Universities (Grant No. 2011QN152).

†Corresponding author. E-mail: chenmbj@sohu.com

© 2013 Chinese Physical Society and IOP Publishing Ltd

PbO, ZnO, $BaCO_3$, K_2CO_3, and Er_2O_3 were used as starting materials. According to the designed composition, certain quantities of starting materials were weighed and well mixed together in an agate mortar. The mixture was placed into an alumina crucible and melted in a muffle furnace at 1100 °C for about 30 min to obtain homogeneously mixed melt. Then, the melted mixture was poured into a preheated brass mold to form glassy samples. After cooling down to room temperature, the samples were cut into several pieces and heat-treated at 450 °C for 10, 20, and 30 min, respectively, in order to grow Ag particles. Finally, the samples were polished carefully to meet the spectral measurements.

2.2. Sample characterization

The glass density was measured according to the Archimedes's principle, using distilled water as the immersion liquid. The Er^{3+} concentrations and mole volumes were estimated based on the designed composition and the measured volumes. The refractive indices were achieved by using a variable angle incidence M-2000 Spectroscopic Ellipsometer (VASE) (J. A. Woollam Co, Inc. USA). The nucleation of Ag particles formed in the glasses was investigated by transmission electron microscope (TEM, JEM-2100, JEOL Ltd. Japan) which functioned with selected area electron diffraction (SAED). The absorption spectra were obtained on a fluorescence spectrophotometer (PC3101, Shimadzu Ltd. Japan) in a range of 300 nm–1750 nm. The emission spectra were measured by a Triax 550 (Jobin Yvon Ltd, France) under excitation of a 488-nm Ar^+ laser. All of the measurements were performed at room temperature.

3. Results and discussion

Figure 1 shows the absorption spectra of Er^{3+}-doped germanate glasses unannealed and annealed at 450 °C for 10, 20, and 30 min. In a measured region from 1225×10^4 cm^{-1} to 3×10^4 cm^{-1}, several sharp absorption peaks corresponding to the transitions from ground state $^4I_{15/2}$ to the excited states $^4G_{11/2}$, $^2H_{9/2}$, $^4F_{7/2,5/2,3/2}$, $^2H_{11/2}$, $^4S_{3/2}$, and $^4F_{9/2}$ of Er^{3+} from high energy side to low energy side are observed. Besides, a broad and strong absorption band centered at around 2.2×10^4 cm^{-1} can also be observed in all of the annealed samples, which corresponds to the absorption of Ag particles due to the SPR of the spatially confined electrons in Ag particles.[28] It can be seen that with the increase of annealing time, the intensity of the plasma oscillation peak increases and the position has a weak red shift, indicating that a lot more Ag particles were formed via long term annealing treatment.

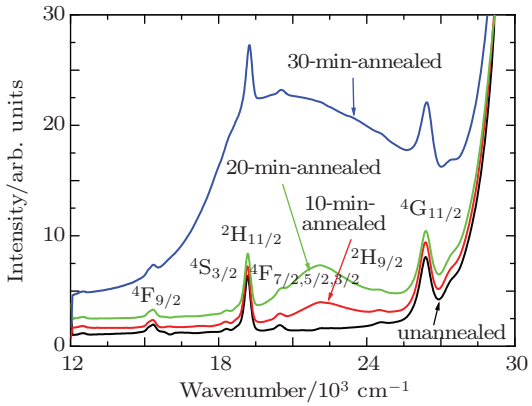


Fig. 1. (color online) Absorption spectra of Er^{3+}-doped gemanate glasses.

In order to evaluate the mean size of Ag particles, the plasmon absorption bands are extracted from the whole absorption spectra, which are shown in Fig. 2 as dotted lines for the glass samples annealed for 10, 20, and 30 min. The sizes of Ag particles are calculated according to the classical light scattering theory by Mie and the free electron theory by Drude,[16] in which the characteristics of the absorption peak are explained as originating from the SPR of metallic particles. According to the Mie–Drude equation, the absorption coefficient can be described as follows:[29]

$$\alpha(\omega) = \frac{9qn^3}{c(1+2n^2)} \frac{\omega^2 \omega_r^2 \tau_c}{(\omega^2 - \omega_r^2)^2 + (\omega_r^2/\omega\tau_c)^2}, \quad (1)$$

where n is the refractive index of the host material, q is the volume fraction of metallic particles, τ_c is the collision time and ω_r is the resonant frequency of the SPs, which can be expressed as

$$\omega_r^2 = \omega_p^2/(1+2n^2), \quad (2)$$

where ω_p is the frequency of plasmon oscillation. Then, upon fitting the SPs? absorption peaks by Eq. (1), the Ag particle size can be obtained as

$$2R = v_f/\Delta\omega_{1/2}, \quad (3)$$

where v_f is the Fermi velocity and equals 1.39×10^8 cm/s,[16] $\Delta\omega_{1/2}$ is the full width at half maximum (FWHM) of the plasmon absorption peak. The fitted curves of SPs? absorptions are depicted in Fig. 2 as solid curves. The theoretical curves show good agreement with the experimental data. Figure 3 shows the dependence of the estimated mean Ag particle size on annealing time. It can be found that when annealing time is 10 min the mean particle size is about 14 nm, and with the further increase of annealing time the mean particle size decreases, indicating a break-down of the Mie–Drude theory due to the assumptions of a smaller distribution of particle sizes and no interaction between particles as Hayakawa *et al*. stated in the study of Eu^{3+}-doped SiO_2 glass containing small Ag particles.[16,29]

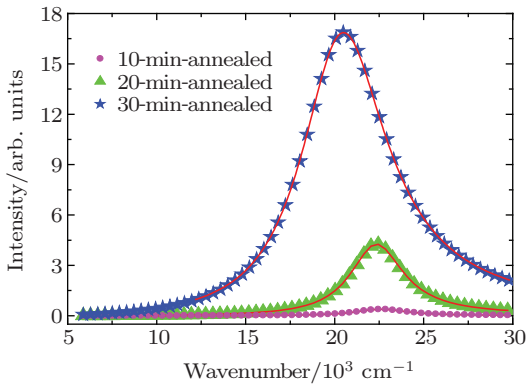


Fig. 2. (color online) Plasmon absorption spectra of Ag particles in Er^{3+}-doped germanate glasses annealed for 10, 20, and 30 min (solid dots: experimental data; solid curves: fitted results).

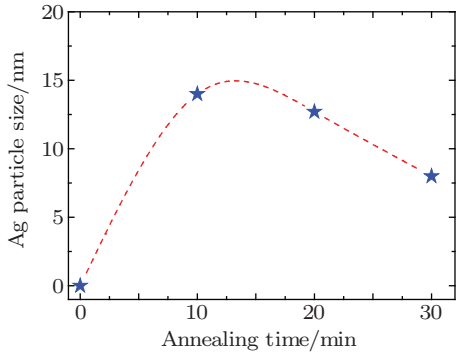
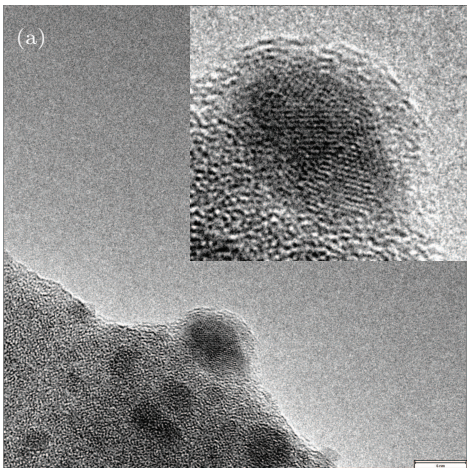


Fig. 3. (color online) Dependence of the estimated mean Ag particle size on the annealing time.

Figure 4(a) shows the TEM image of Er^{3+}-doped germanate glass containing Ag particles annealed at 450 °C for 20 min. Some dark areas whose compositions are different from those in most parts of the sample are observed in the TEM image. The inset in the top right corner in Fig. 4(a) shows an enlarged image of a typical dark area. It can be seen that a lot of atoms are arranged regularly in the dark area but not in the full dark area. In order to identify the particles, the selected area electron-diffraction SAED pattern is taken and is shown in Fig. 4(b). From the SAED image, the crystal plane distance is calculated to be 2.359 Å (1 Å=0.1 nm) which is in agreement with the value of (111) plane of metal Ag, indicating that the dark area in Fig. 4(a) corresponds to Ag particles. The average particle size estimated from Fig. 4(a) is about 5 nm, which is smaller than the value calculated by Mie–Drude theory. The difference between the particle sizes derived from the above two routes is due to the fact that the Mie–Drude theory is established on the ideal case that the metal particles possess regularly spherical shape and the size distribution is localized in a narrow region. That is to say, the mean particle size estimated from the Mie–Drude theory deviates from the real value. However, the results of the particle sizes obtained from the Mie–Drude theory can reflect the variation trend of the real particle sizes.



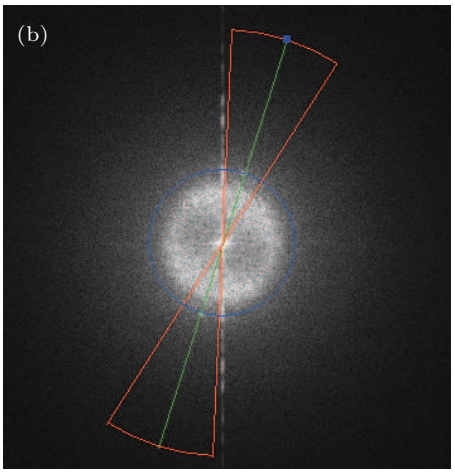


Fig. 4. (color online) TEM pattern (cross section) of Ag particles formed after annealing at 450 °C for 20 min. (a) TEM pattern, (b) selected area electron-diffraction pattern.

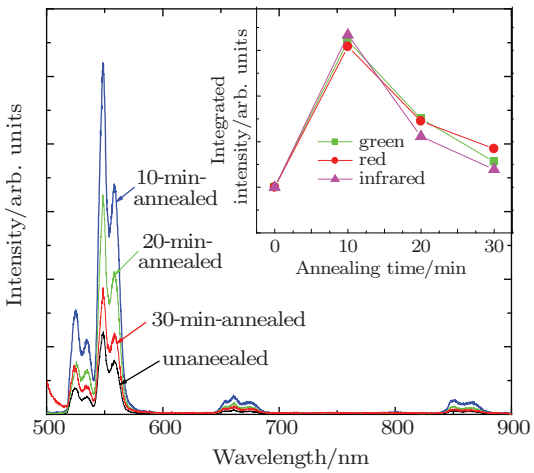


Fig. 5. (color online) Fluorescence spectra of Er^{3+} in germanate glasses excited by 488-nm Ar^+ laser, with the inset showing the correlation of the integrated fluorescence intensities of green, red, and infrared emissions with the annealing time.

Figure 5 shows the fluorescence spectra of Er^{3+}-doped germanate glasses excited by 488-nm Ar^+ ion laser and measured under identical experimental conditions. It can be found that three emission bands in the green (510 nm–580 nm), red

(640 nm–680 nm), and infrared (840 nm–870 nm) regions are observed, which can be assigned to $(^2H_{11/2}, {}^4S_{3/2}) \rightarrow {}^4I_{15/2}$, ${}^4F_{9/2} \rightarrow {}^4I_{15/2}$, and ${}^4S_{3/2} \rightarrow {}^4I_{13/2}$ transitions of Er^{3+}, respectively. It should be noted that an emission enhancement is observed for all the annealed samples compared with the unannealed one. When the annealing time increases up to 10 min, the emission intensity reaches a maximum value, which is almost 4.2 times higher than that of the unannealed one without Ag particles. With the further increase of the annealing time, the emission intensity decreases dramatically but it is still higher than the unannealed one. The inset of Fig. 5 shows the dependences of the integrated fluorescence intensities of green, red, and infrared emissions on the annealing time.

From the above results, it cannot be deduced whether the fluorescence enhancement is induced by the SPR. In fact, the mechanisms of fluorescence enhancement can be multifold. On the one hand, the change of fluorescence intensity may result from the enhanced pump absorption by the plasmon oscillation; on the other hand, it can also be caused by the field enhancement effect; moreover the crystal field change evoked by the post-heat treatment can possibly lead to the fluorescence enhancement. To verify the origination of fluorescence enhancement, the quotient spectra $R(\lambda)$ of different samples are derived from the formula $R(\lambda) = I_{\text{annealed}}(\lambda)/I_{\text{unannealed}}(\lambda)$ based on the fluorescence spectra in Fig. 5, where $I_{\text{annealed}}(\lambda)$ and $I_{\text{unannealed}}(\lambda)$ are the normalized fluorescence intensities for the annealed samples and the unannealed one in a wavelength range from 500 nm to 900 nm. Figure 6 shows the quotient spectra, where three smooth straight lines in the regions of emission bands corresponding to $(^2H_{11/2}, {}^4S_{3/2}) \rightarrow {}^4I_{15/2}$, ${}^4F_{9/2} \rightarrow {}^4I_{15/2}$, and ${}^4S_{3/2} \rightarrow {}^4I_{13/2}$ transitions of Er^{3+} are presented, indicating no obvious change in the emission spectral profile of Er^{3+} after the formation of Ag particles by post-annealing treatment. Therefore, it can be concluded that the introduction of Ag particles in Er^{3+}-doped germanate glass has no effect on the crystal field environment of Er^{3+}, while it only induces the enhancement of the emission intensity.

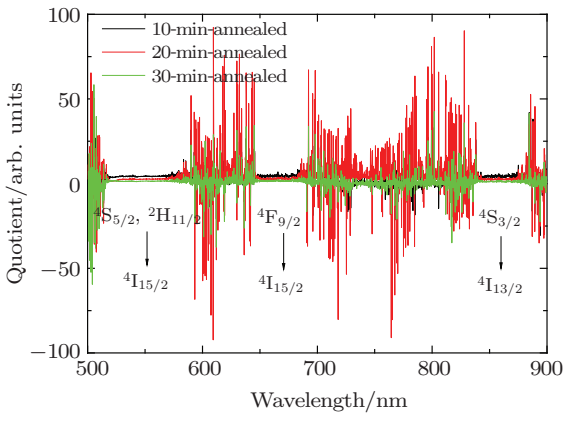


Fig. 6. (color online) The quotient spectra of the fluorescence spectra ranging from 500 nm to 900 nm of Er^{3+} in germanate glasses annealed for 10, 20, and 30 min.

To further check the influence of heat treatment on the optical transition properties of Er^{3+}, Judd–Ofelt calculations are performed in the framework of three parameters based on the Judd–Ofelt theory,[30,31] which was developed independently by Brian Judd and George Ofelt in 1962 and has been widely used in the spectroscopic studies related to f–f transitions of rare-earth ions. Based on their theory, the oscillator strength f_{ed} for an electric-dipole transition between two $4f$ levels of rare-earth ions can be written as

$$f_{\text{ed}} = \frac{8\pi^2 mc\nu}{3h(2J+1)} \frac{(n^2+2)^2}{9n} \sum_{\lambda=2,4,6} \Omega_\lambda \left(\langle \Psi J | \left| U^\lambda \right| | \Psi' J' \rangle \right)^2. \tag{4}$$

The oscillator strength f_{md} for a magnetic dipole transition can be expressed as

$$f_{\text{md}} = \frac{h\nu n}{6mc(2J+1)} \left| \langle \Psi J | | L + 2S | | \Psi' J' \rangle \right|^2. \tag{5}$$

In Eqs. (4) and (5), m is the mass of electron, c is the speed of light, ν is the wavenumber for the studied transition, n represents the refractive index of the host, h refers to the Planck constant, J is the angular moment of the initial state, Ω_λ ($\lambda = 2, 4, 6$) are the three intensity parameters, namely, Judd–Ofelt intensity parameters, and $\langle \Psi J | \left| U^\lambda \right| | \Psi' J' \rangle$ and $\langle \Psi J \| L + 2S \| \Psi' J' \rangle$ are the reduced matrix elements for electric and magnetic dipole transitions, respectively. The experimental oscillator strength for an absorption transition at wavenumber ν can be calculated according to the absorption cross section by using the following equation

$$f_{\text{ex}} = \frac{mc}{\pi e^2} \int \sigma(\nu) \mathrm{d}\nu, \tag{6}$$

where $\sigma(\nu)$ represents the absorption cross section at wavenumber ν and can be determined from the following equation

$$\sigma(\nu) = \frac{\ln[I_0(\nu)/I(\nu)]}{Nt}, \tag{7}$$

where $I_0(\nu)$ and $I(\nu)$ are the incident light intensity and the output light intensity, N is the number of rare-earth ions per unit volume, and t is the thickness of the sample. The calculated absorption cross sections from the absorption spectra by using Eq. (7) are shown in Fig. 7. The intrinsic transitions of Er^{3+} from ground state ${}^4I_{15/2}$ to the excited states ${}^4I_{13/2}$, ${}^4I_{11/2}$, ${}^4I_{9/2}$, ${}^4F_{9/2}$, ${}^4S_{3/2}$, ${}^2H_{11/2}$, ${}^4F_{7/2}$, ${}^4F_{5/2,3/2}$, ${}^2H_{9/2}$, and ${}^4G_{11/2}$ are observed. For each absorption transition, the barycenter wavenumber is calculated from the following formula

$$\bar{\nu} = \frac{\int \sigma(\nu) \nu \mathrm{d}\nu}{\int \sigma(\nu) \mathrm{d}\nu}. \tag{8}$$

The experimental oscillator strengths are derived from Eqs. (4) and (5). The Judd–Ofelt intensity parameters of Er^{3+} in unannealed and annealed samples are calculated via the least squares method by using Eqs. (4)–(6) and are shown in the last row of Table 1. The theoretical oscillator strengths are

obtained from Eq. (6). For comparison, all the calculated results for the samples unannealed and annealed for 20 min are listed in Table 1. The calculation errors are estimated according to the following formula

$$\delta = \sqrt{\frac{\sum_i (f_{\rm ex}^i - f_{\rm th}^i)^2}{M-3}}, \tag{9}$$

where i presents the i-th transition, M is the number of involved transitions, $f_{\rm ex}^i - f_{\rm th}^i$ represents the difference between theoretical and experimental oscillator strengths. From Table 1 it can be seen that the calculation errors are rather small, and that the optical transition intensity parameters for both the samples are very similar. This means that the Judd–Ofelt calculations are reliable; meanwhile the introduction of Ag particles does not bring obvious influence on the optical transition properties of Er^{3+} in the glass. Thus, we can be sure that the fluorescence enhancement of Er^{3+} is not due to the change of radiative transition properties of Er^{3+} in germanate glass.

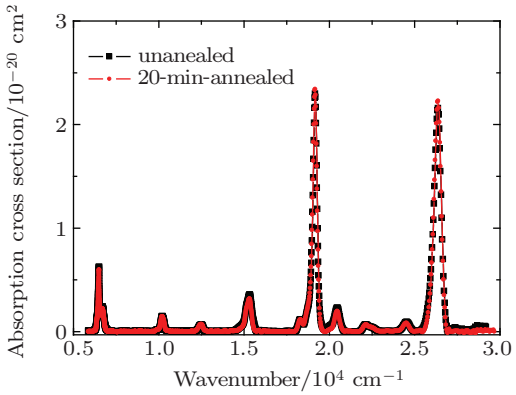


Fig. 7. (color online) Absorption cross section of Er^{3+} in unannealed and 20-min-annealed samples.

Table 1. Peak wavenumber values of absorption cross-section, the experimental and the theoretical oscillator strengths of absorption transitions, and the Judd–Ofelt intensity parameters of Er^{3+} in unannealed and 20-min-annealed samples.

Energy level	Barycentre wavenumber/cm^{-1}		Oscillator strengths ($\times 10^{-6}$)			
			unannealed		20-min-annealed	
	unannealed	20-min-annealed	Experimental	Theoretical	Experimental	Theoretical
$^4I_{13/2}$	6544.9	6545.3	145.01	87.86 (ed) 54.02 (md)	143.84	87.64 (ed) 53.38 (md)
$^4I_{11/2}$	9965.6	9959.8	43.83	44.61	43.25	44.89
$^4I_{9/2}$	12332.9	12331.7	22.55	31.83	27.12	30.28
$^4F_{9/2}$	15214.9	15214.1	191.25	184.75	181.49	178.34
$^4S_{3/2}$	18327.3	18330.3	34.3	29.66	34.92	29.8
$^2H_{11/2}$	19131.4	19131.7	896.34	935.85	900.86	938.71
$^4F_{7/2}$	20598.0	20596.1	118.35	142.07	123.03	140.09
$^4F_{5/2,3/2}$	22357.2	22355.5	44.55	56.54	44.83	56.79
$^2H_{9/2}$	24623.6	24621.8	48.75	47.99	47.62	47.69
$^4G_{11/2}$	26311.5	26311.7	1341.15	1287.08	1342.91	1291
unannealed/10^{-20} cm^2: $\Omega_2 = 5.49$, $\Omega_4 = 1.50$, $\Omega_6 = 0.69$. Error: $\delta = 27.65 \times 10^{-6}$						
20-min-annealed/10^{-20} cm^2: $\Omega_2 = 5.65$, $\Omega_4 = 1.45$, $\Omega_6 = 0.70$. Error: $\delta = 25.68 \times 10^{-6}$						

It has been reported that when the distances between heavy metal particles and the neighboring particles are not more than 10 nm, a 100 times more intense electromagnetic near-field induced by the SPR can be obtained compared with by the direct excitation in a plasmon-free case.[27] Since the interaction distance between SPs and rare-earth ions is far larger than the coordinate space of 4f electron wave functions of rare-earth ions, the fluorescence enhancement can be obtained by the SPR excitation. Furthermore, considering that there is no resonant absorption of Er^{3+} at 488 nm, we deduce that the mechanism for the fluorescence enhancement in our experiments is the local field enhancement effect around Er^{3+} induced by the SPR of Ag particles.[16]

4. Conclusions

Er^{3+}-doped germanate glasses containing Ag particles were prepared via a melt-quenching technique with post-annealing treatment. The results of TEM and optical absorption spectra confirm the formation of Ag particles via the post-annealing treatment. The fluorescence intensities of all the annealed samples containing Ag particles each have an enhancement compared with that of the unannealed one. The quotient spectra of the fluorescence spectra are calculated and confirm that all of the emission spectra have the same profiles, indicating that the crystal field environment of Er^{3+} occupied sites is unchanged. The optical transition properties are studied in the framework of Judd–Ofelt theory. It is found that the absorption cross-section range from 6×10^3 cm^{-1} to 3×10^4 cm^{-1} and optical transition intensity parameters are almost unchanged

no matter whether there are Ag parties in the glass. The results indicate that the introduction of Ag particles has no influence on radiative transition property of Er^{3+}. Thus, the most probable mechanism for the observed fluorescence enhancement is the field enhancement effect induced by the SPR of Ag particles in germanate glass.

References

[1] Zhang H Y, Yang L Q, Meng L, Nie J C, Ning T Y, Liu W M, Sun J Y and Wang P F 2012 *Chin. Phys.* B **21** 020601

[2] Wu D J, Jiang S M and Liu X J 2012 *Chin. Phys.* B **21** 077803

[3] Nie S M and Emory S R 1997 *Science* **275** 1102

[4] Dintinger J, Klein S and Ebbesen T W 2006 *Adv. Mater.* (Weinheim, Ger.) **18** 1267

[5] Zhou F, Liu Y and Li Z Y 201 *Chin. Phys*. B **20** 037303

[6] Schaadt D M, Feng B and Yu E T 2005 *Appl. Phys. Lett.* **86** 063106

[7] Okamoto K, Niki I, Shvartser A, Narukawa Y, Mukai T and Scherer A 2004 *Nature Mater.* **3** 601

[8] Shi X Z, Shen C M, Wang D K, Li C, Tian Y, Xu Z C, Wang C M and Gao H J 2011 *Chin. Phys.* B **20** 076103

[9] Okamoto K, Niki I, Scherer A, Narukawa Y, Mukai T and Kawakami Y 2005 *Appl. Phys. Lett.* **87** 071102

[10] Qiu D J, Fan W Z, Weng S, Wu H Z and Wang J 2011 *Acta Phys. Sin*. **60** 087301 (in Chinese)

[11] Xiao C W, Shen C M, Yang T Z, Gao H J and Xu Z C 2008 *Chin. Phys.* B **17** 2066

[12] Wang X T, Shi W S, She G W, Mu L X and Lee S T 2010 *Appl. Phys. Lett.* **96** 053104

[13] Pompa P P, Martiradonna L, Della Torre A, Della SaLa F, Manna L, De Vittorio M, Calabi F, Cingolani R and Rinaldi R 2006 *Nature* **444** 126

[14] Joseph R L 2004 *Anal. Biochem.* **324** 153

[15] Popov O, Lirtsman V and Davidov D 2009 *Appl. Phys. Lett.* **95** 191108

[16] Tomokatsu H, Selvan S and Nogami M 1999 *Appl. Phys. Lett.* **74** 1513

[17] Strohhofer C and Polman A 2002 *Appl. Phys. Lett.* **81** 1414

[18] Wang C H, Chen C W, Chen Y T, Wei C M, Chen Y F, Lai C W, Ho M L, Chou P T and Hofmann M 2010 *Appl. Phys. Lett.* **96** 071906

[19] Duan L, Lin B X, Zhang W, Zhong S and Fu Z X 2006 *Appl. Phys. Lett.* **88** 232110

[20] Malta O L, Santa-Cruz P A, De Sá G F and Auzel F 1985 *J. Lumin.* **33** 261

[21] Jimenez J, Lysenko S and Liu H 2008 *J. Appl. Phys.* **104** 054313

[22] Mertens H and Polman A 2006 *Appl. Phys. Lett.* **89** 211107

[23] Wu Y, Xu T F, Shen X, Dai S X, Nie Q H, Wang X S, Song B A, Zhang W and Lin C G 2011 6*th IEEE Conference on Industrial Electronics and Applications* (ICIEA), June 21–23, Beijing China, p. 1464

[24] Bomfim F A, Martinelli J R, Kassab L R P, Assumpção T A A and de Araújo C B 2010 *J. Non-Cryst. Solids* **356** 2598

[25] Rivera V A G, Osorio S P A, Ledemi Y, Manzani D, Messaddeq Y, Nunes L A O and Marega E 2010 *Opt. Express* **18** 25321

[26] Liu C and Heo J 2010 *J. Am. Ceram. Soc.* **93** 3349

[27] Eichelbaum M and Rademann K 2009 *Adv. Func. Mater.* **19** 2045

[28] Doremus R H 1965 *J. Chem. Phys*. **42** 414

[29] Hayakawa T, Selvan S T and Nogami M 1999 *J. Non-Cryst. Solids* **259** 16

[30] Ofelt G S 1962 *J. Chem. Phys.* **37** 511

[31] Judd B R 1962 *Phys. Rev.* **127** 750